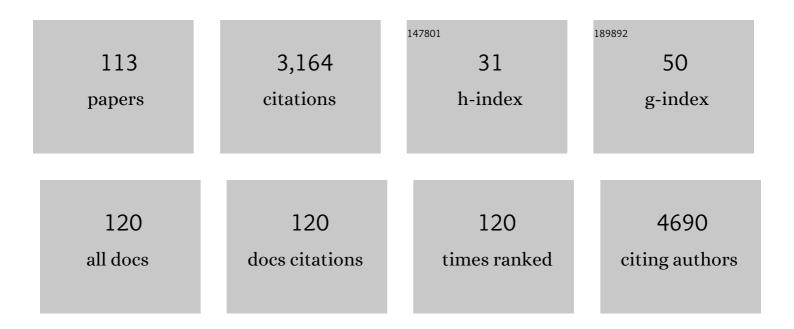
Magdalena Parlinska-Wojtan

List of Publications by Year in descending order

Source: https://exaly.com/author-pdf/431402/publications.pdf Version: 2024-02-01



#	Article	IF	CITATIONS
1	Highly Active and Stable Single-Atom Cu Catalysts Supported by a Metal–Organic Framework. Journal of the American Chemical Society, 2019, 141, 5201-5210.	13.7	361
2	Applications of Noble Metal-Based Nanoparticles in Medicine. International Journal of Molecular Sciences, 2018, 19, 4031.	4.1	172
3	Characterization of Silver Nanoparticle Products Using Asymmetric Flow Field Flow Fractionation with a Multidetector Approach – a Comparison to Transmission Electron Microscopy and Batch Dynamic Light Scattering. Analytical Chemistry, 2012, 84, 2678-2685.	6.5	142
4	FTIR-ATR spectroscopy of pollen and honey as a tool for unifloral honey authentication. The case study of rape honey. Food Control, 2018, 84, 33-40.	5.5	99
5	Encapsulation of Ru nanoparticles: Modifying the reactivity toward CO and CO2 methanation on highly active Ru/TiO2 catalysts. Applied Catalysis B: Environmental, 2020, 270, 118846.	20.2	84
6	Lattice dynamics of NiTi austenite, martensite, andRphase. Physical Review B, 2002, 66, .	3.2	83
7	Green synthesis and antibacterial effects of aqueous colloidal solutions of silver nanoparticles using camomile terpenoids as a combined reducing and capping agent. Bioprocess and Biosystems Engineering, 2016, 39, 1213-1223.	3.4	80
8	Deactivation of Au/CeO2 catalysts during CO oxidation: Influence of pretreatment and reaction conditions. Journal of Catalysis, 2016, 341, 160-179.	6.2	67
9	Raising the CO _{<i>x</i>} Methanation Activity of a Ru/γâ€Al ₂ O ₃ Catalyst by Activated Modification of Metal–Support Interactions. Angewandte Chemie - International Edition, 2020, 59, 22763-22770.	13.8	66
10	Microstructure and mechanical properties of Al–Si–N transparent hard coatings deposited by magnetron sputtering. Surface and Coatings Technology, 2007, 202, 884-889.	4.8	62
11	Varied-shaped gold nanoparticles with nanogram killing efficiency as potential antimicrobial surface coatings for the medical devices. Scientific Reports, 2021, 11, 12546.	3.3	61
12	Controlling the O-Vacancy Formation and Performance of Au/ZnO Catalysts in CO ₂ Reduction to Methanol by the ZnO Particle Size. ACS Catalysis, 2021, 11, 9022-9033.	11.2	53
13	Nanocrystalline-to-amorphous transition in nanolaminates grown by low temperature atomic layer deposition and related mechanical properties. Applied Physics Letters, 2012, 100, .	3.3	52
14	In-situ SEM indentation studies of the deformation mechanisms in TiN, CrN and TiN/CrN. Micron, 2009, 40, 22-27.	2.2	50
15	Morphological, structural and mechanical properties of NbN thin films deposited by reactive magnetron sputtering. Surface and Coatings Technology, 2006, 200, 6544-6548.	4.8	49
16	Microstructure and nanohardness properties of Zr–Al–N and Zr–Cr–N thin films. Journal of Vacuum Science and Technology A: Vacuum, Surfaces and Films, 2005, 23, 593-598.	2.1	47
17	CO ₂ Reduction to Methanol on Au/CeO ₂ Catalysts: Mechanistic Insights from Activation/Deactivation and SSITKA Measurements. ACS Catalysis, 2020, 10, 3580-3594.	11.2	47
18	In vitro studies of the adhesion of diamond-like carbon thin films on CoCrMo biomedical implant alloy. Acta Materialia, 2011, 59, 4678-4689.	7.9	44

#	Article	IF	CITATIONS
19	Effects of laser surface texturing on the wear and failure mechanism of grey cast iron reciprocating against steel under starved lubrication conditions. Wear, 2017, 386-387, 29-38.	3.1	44
20	FTIR analysis of molecular composition changes in hazel pollen from unpolluted and urbanized areas. Aerobiologia, 2017, 33, 1-12.	1.7	43
21	Characterization of thermally treated TiAlSiN coatings by TEM and nanoindentation. Surface and Coatings Technology, 2004, 188-189, 344-350.	4.8	42
22	Analysis of morphological and molecular composition changes in allergenic Artemisia vulgaris L. pollen under traffic pollution using SEM and FTIR spectroscopy. Environmental Science and Pollution Research, 2016, 23, 23203-23214.	5.3	42
23	Plastic deformation modes of gallium arsenide in nanoindentation and nanoscratching. Applied Physics Letters, 2007, 90, 031902.	3.3	41
24	Spectroscopic assessment of the role of hydrogen in surface defects, in the electronic structure and transport properties of TiO ₂ , ZnO and SnO ₂ nanoparticles. Physical Chemistry Chemical Physics, 2013, 15, 1417-1430.	2.8	40
25	Phospholipid-protein balance in affective disorders: Analysis of human blood serum using Raman and FTIR spectroscopy. A pilot study. Journal of Pharmaceutical and Biomedical Analysis, 2016, 131, 287-296.	2.8	40
26	ROS-Mediated Apoptosis and Autophagy in Ovarian Cancer Cells Treated with Peanut-Shaped Gold Nanoparticles. International Journal of Nanomedicine, 2021, Volume 16, 1993-2011.	6.7	40
27	Conventional and high resolution TEM investigation of the microstructure of compositionally graded TiAlSiN thin films. Surface and Coatings Technology, 2004, 177-178, 376-381.	4.8	37
28	CO2 hydrogenation on a metal hydride surface. Physical Chemistry Chemical Physics, 2012, 14, 5518.	2.8	37
29	Exchange Bias and Domain Evolution at 10Ânm Scales. Physical Review Letters, 2010, 105, 197201.	7.8	36
30	Effect of Nb doping on structural, optical and photocatalytic properties of flame-made TiO2 nanopowder. Environmental Science and Pollution Research, 2012, 19, 3696-3708.	5.3	36
31	Effect of Si incorporation on the properties of niobium nitride films deposited by DC reactive magnetron sputtering. Surface and Coatings Technology, 2004, 188-189, 435-439.	4.8	33
32	Identification of birch pollen species using FTIR spectroscopy. Aerobiologia, 2018, 34, 525-538.	1.7	33
33	Microstructural comparison of material damage in GaAs caused by Berkovich and wedge nanoindentation and nanoscratching. Scripta Materialia, 2008, 59, 364-367.	5.2	30
34	Temperature dependence of large exchange-bias in TbFe-Co/Pt. Applied Physics Letters, 2012, 101, .	3.3	30
35	Sequence of deformation and cracking behaviours of Gallium–Arsenide during nano-scratching. Materials Chemistry and Physics, 2013, 138, 38-48.	4.0	30
36	Green synthesis and antibacterial effects of aqueous colloidal solutions of silver nanoparticles using clove eugenol. Applied Organometallic Chemistry, 2018, 32, e4276.	3.5	29

#	Article	IF	CITATIONS
37	Effects of SiO2-doping on high-surface-area Ru/TiO2 catalysts for the selective CO methanation. Applied Catalysis B: Environmental, 2021, 282, 119483.	20.2	27
38	Synthesis and catalytic, antimicrobial and cytotoxicity evaluation of gold and silver nanoparticles using biodegradable, Î-conjugated polyamic acid. Environmental Science: Nano, 2015, 2, 518-527.	4.3	26
39	Fe ₃ O ₄ @SiO ₂ @Au nanoparticles for MRI-guided chemo/NIR photothermal therapy of cancer cells. RSC Advances, 2020, 10, 26508-26520.	3.6	26
40	Bactericidal Properties of Rod-, Peanut-, and Star-Shaped Gold Nanoparticles Coated with Ceragenin CSA-131 against Multidrug-Resistant Bacterial Strains. Pharmaceutics, 2021, 13, 425.	4.5	25
41	Steering the selectivity in CO2 reduction on highly active Ru/TiO2 catalysts: Support particle size effects. Journal of Catalysis, 2021, 401, 160-173.	6.2	25
42	Effect of tantalum addition on microstructure and optical properties of TiN thin films. Thin Solid Films, 2007, 515, 6758-6764.	1.8	23
43	The role of zinc deficiency-induced changes in the phospholipid-protein balance of blood serum in animal depression model by Raman, FTIR and UV–vis spectroscopy. Biomedicine and Pharmacotherapy, 2017, 89, 549-558.	5.6	22
44	Design and assembly of ternary Pt/Re/SnO2 NPs by controlling the zeta potential of individual Pt, Re, and SnO2 NPs. Journal of Nanoparticle Research, 2018, 20, 144.	1.9	22
45	The influence of the grain boundary phase on the mechanical properties of Si3N4–MoSi2 composites. Acta Materialia, 2007, 55, 2875-2884.	7.9	21
46	Structural anelasticity of NiTi during two-stage martensitic transformation. Journal of Alloys and Compounds, 2000, 310, 312-317.	5.5	20
47	Transmission electron microscopy characterization of TiN/SiNx multilayered coatings plastically deformed by nanoindentation. Thin Solid Films, 2010, 518, 4890-4897.	1.8	20
48	Platinum–gold nanoraspberries as effective photosensitizer in anticancer photothermal therapy. Journal of Nanobiotechnology, 2019, 17, 107.	9.1	20
49	Size effect of platinum nanoparticles in simulated anticancer photothermal therapy. Photodiagnosis and Photodynamic Therapy, 2020, 29, 101594.	2.6	20
50	From spherical to bone-shaped gold nanoparticles—Time factor in the formation of Au NPs, their optical and photothermal properties. Photodiagnosis and Photodynamic Therapy, 2020, 30, 101670.	2.6	20
51	Nanoindentation deformation and cracking in sapphire. Ceramics International, 2019, 45, 9835-9845.	4.8	19
52	In situ scanning electron microscopy indentation studies on multilayer nitride films: Methodology and deformation mechanisms. Journal of Materials Research, 2009, 24, 1208-1221.	2.6	18
53	Preparation of Pt-skin PtRhNi Nanoframes Decorated with Small SnO ₂ Nanoparticles as an Efficient Catalyst for Ethanol Oxidation Reaction. ACS Applied Materials & Interfaces, 2019, 11, 22352-22363.	8.0	18
54	Oxygen diffusion in columnar TiAlSiN coatings investigated by electron microscopy. Thin Solid Films, 2016, 616, 437-443.	1.8	17

#	Article	IF	CITATIONS
55	Olfactory bulbectomy-induced changes in phospholipids and protein profiles in the hippocampus and prefrontal cortex of rats. A preliminary study using a FTIR spectroscopy. Pharmacological Reports, 2016, 68, 521-528.	3.3	17
56	Structural, chemical and optical properties of SnO 2 NPs obtained by three different synthesis routes. Journal of Physics and Chemistry of Solids, 2017, 107, 100-107.	4.0	17
57	Temperature-controlled synthesis of hollow, porous gold nanoparticles with wide range light absorption. Journal of Materials Science, 2020, 55, 5257-5267.	3.7	17
58	Phase constitution and interface structure of nano-sized Ag-Cu/AlN multilayers: Experiment and <i>ab initio</i> modeling. Applied Physics Letters, 2012, 101, .	3.3	16
59	Comparing dried and liquid blood serum samples of depressed patients: An analysis by Raman and infrared spectroscopy methods. Journal of Pharmaceutical and Biomedical Analysis, 2018, 150, 80-86.	2.8	16
60	Influence of Ge addition on the morphology and properties of TiN thin films deposited by magnetron sputtering. Thin Solid Films, 2006, 496, 336-341.	1.8	15
61	Nanocomposite Al–Ge–N thin films and their mechanical and optical properties. Journal of Materials Chemistry, 2012, 22, 16761.	6.7	15
62	Mechanical and tribological properties of polymer-derived Si/C/N sub-millimetre thick miniaturized components fabricated by direct casting. Journal of the European Ceramic Society, 2012, 32, 1759-1767.	5.7	15
63	Synthesis and characterization of new functionalized polymer-Fe3O4 nanocomposite particles. EXPRESS Polymer Letters, 2017, 11, 2-13.	2.1	15
64	Fancy-Shaped Gold–Platinum Nanocauliflowers for Improved Proton Irradiation Effect on Colon Cancer Cells. International Journal of Molecular Sciences, 2020, 21, 9610.	4.1	15
65	Passing the limit of electrodeposition: †Gas template' H2 nanobubbles for growing highly crystalline nanoporous ZnO. Nano Energy, 2012, 1, 742-750.	16.0	14
66	Ternary Pt/Re/SnO2/C catalyst for EOR: Electrocatalytic activity and durability enhancement. Nano Research, 2020, 13, 832-842.	10.4	14
67	FePt films on self-assembled SiO2 particle arrays. Journal of Applied Physics, 2008, 103, 053903.	2.5	13
68	Qualitative and quantitative changes in phospholipids and proteins investigated by spectroscopic techniques in olfactory bulbectomy animal depression model. Journal of Pharmaceutical and Biomedical Analysis, 2018, 148, 24-31.	2.8	13
69	Rod-shaped gold nanoparticles exert potent candidacidal activity and decrease the adhesion of fungal cells. Nanomedicine, 2020, 15, 2733-2752.	3.3	13
70	Application of iron-based magnetic nanoparticles stabilized with triethanolammonium oleate for theranostics. Journal of Materials Science, 2022, 57, 4716-4737.	3.7	13
71	Differential of cholangiocarcinoma disease using Raman spectroscopy combined with multivariate analysis. Spectrochimica Acta - Part A: Molecular and Biomolecular Spectroscopy, 2022, 272, 121006.	3.9	13
72	Correlation of electrolyte-derived inclusions to crystallization in the early stage of anodic oxide film growth on titanium. Thin Solid Films, 2012, 520, 1804-1808.	1.8	12

#	Article	IF	CITATIONS
73	Control of Arms of Au Stars Size and its Dependent Cytotoxicity and Photosensitizer Effects in Photothermal Anticancer Therapy. International Journal of Molecular Sciences, 2019, 20, 5011.	4.1	12
74	Conversion of bimetallic PtNi ₃ nanopolyhedra to ternary PtNiSn nanoframes by galvanic replacement reaction. Nanoscale, 2019, 11, 5355-5364.	5.6	12
75	The optimization of methods of synthesis of nickel–silver core–shell nanoparticles for conductive materials. Nanotechnology, 2019, 30, 015601.	2.6	12
76	Qualitative and quantitative changes in phospholipids and proteins investigated by spectroscopic techniques in animal depression model. Spectrochimica Acta - Part A: Molecular and Biomolecular Spectroscopy, 2017, 176, 30-37.	3.9	11
77	Synthesis methodâ€dependent photothermal effects of colloidal solutions of platinum nanoparticles used in photothermal anticancer therapy. Applied Organometallic Chemistry, 2020, 34, e5401.	3.5	11
78	Exploiting interactions between structure size and indentation size effects to determine the characteristic dimension of nano-structured materials by indentation. Journal Physics D: Applied Physics, 2013, 46, 265301.	2.8	10
79	Distributed Bragg reflectors obtained by combining Se and Te compounds: Influence on the luminescence from CdTe quantum dots. Journal of Applied Physics, 2016, 119, 183105.	2.5	9
80	Ternary Pt/Re/SnO2 nanoparticles for ethanol oxidation reaction: Understanding the correlation between the synthesis route and the obtained material. Applied Catalysis A: General, 2019, 570, 319-328.	4.3	8
81	Gold nanodahlias: potential nanophotosensitizer in photothermal anticancer therapy. Journal of Materials Science, 2020, 55, 2530-2543.	3.7	8
82	Influence of intergranular phases on edge integrity of Si3N4/SiC wood cutting tools. Journal of the European Ceramic Society, 2011, 31, 2711-2719.	5.7	7
83	AlN/Si 3 N 4 multilayers as an interface model system for Al 1â^'x Si x N/Si 3 N 4 nanocomposite thin films. Surface and Coatings Technology, 2015, 261, 418-425.	4.8	7
84	Design and Control of Mode Interaction in Coupled ZnTe Optical Microcavities. Crystal Growth and Design, 2017, 17, 3716-3723.	3.0	7
85	Gold Nanopeanuts as Prospective Support for Cisplatin in Glioblastoma Nano-Chemo-Radiotherapy. International Journal of Molecular Sciences, 2020, 21, 9082.	4.1	7
86	Gold-Decorated Platinum and Palladium Nanoparticles as Modern Nanocomplexes to Improve the Effectiveness of Simulated Anticancer Proton Therapy. Pharmaceutics, 2021, 13, 1726.	4.5	7
87	Controlling the selectivity of high-surface-area Ru/TiO2 catalysts in CO2 reduction - modifying the reaction properties by Si doping of the support. Applied Catalysis B: Environmental, 2022, 317, 121748.	20.2	7
88	Adaptive composites with embedded NiTiCu wires. , 2001, 4333, 377.		6
89	Differences in Electrophysical and Gas Sensing Properties of Flame Spray Synthesized Fe ₂ O ₃ (<i>î³</i> -Fe ₂ O ₃ and) Tj ETQq1 1 0.784314 rgBT /Ove 6401-6411.	erlock 10 T 0.9	rf 50 102 Td
90	Effect of electron-hole separation on optical properties of individual Cd(Se,Te) quantum dots. Physical Review B, 2016, 93, .	3.2	6

#	Article	IF	CITATIONS
91	<title>Shape memory alloy wires turn composites into smart structures: II. Manufacturing and properties</title> . , 2002, , .		5
92	Microstructure and reducibility of Ce–Er–O mixed oxides supported on γ-Al2O3 – Effect of preparation method. Applied Surface Science, 2015, 351, 1094-1104.	6.1	5
93	Phonons in austenite and martensite NiTi crystals. European Physical Journal Special Topics, 2003, 112, 635-638.	0.2	5
94	Real space crystallography of a complex metallic alloy: high-angle annular dark-field scanning transmission electron microscopy of o-Al ₄ (Cr,Fe). Journal of Applied Crystallography, 2014, 47, 1026-1031.	4.5	5
95	Peanut-Shaped Gold Nanoparticles with Shells of Ceragenin CSA-131 Display the Ability to Inhibit Ovarian Cancer Growth In Vitro and in a Tumor Xenograft Model. Cancers, 2021, 13, 5424.	3.7	5
96	Ceragenin-Coated Non-Spherical Gold Nanoparticles as Novel Candidacidal Agents. Pharmaceutics, 2021, 13, 1940.	4.5	5
97	The role of the addition of Cu in alloyed and multilayered Fe-based nanowires. Materials Science and Engineering B: Solid-State Materials for Advanced Technology, 2022, 281, 115732.	3.5	5
98	Structural investigation of SnO ₂ catalytic nanoparticles doped with F and Sb. Surface and Interface Analysis, 2014, 46, 1090-1093.	1.8	4
99	Mechanical behavior of intragranular, nano-porous electrodeposited zinc oxide. Thin Solid Films, 2015, 578, 174-179.	1.8	4
100	3D π-Conjugated Poly(amic) Acid Polymer as Support Matrices for Ethanol Electro-Oxidation on Palladium and Platinum Catalysts. Electrocatalysis, 2016, 7, 317-325.	3.0	4
101	Ultraslow Spin Relaxation Dynamics in Colloidal Copper-Doped CdSe Quantum Dots. Journal of Physical Chemistry C, 2020, 124, 1042-1052.	3.1	4
102	Similarities in the General Chemical Composition of Colon Cancer Cells and Their Microvesicles Investigated by Spectroscopic Methods-Potential Clinical Relevance. International Journal of Molecular Sciences, 2020, 21, 1826.	4.1	4
103	Targeting bacteria causing otitis media using nanosystems containing nonspherical gold nanoparticles and ceragenins. Nanomedicine, 2021, 16, 2657-2678.	3.3	4
104	N-Acetyl-Cysteine Increases Activity of Peanut-Shaped Gold Nanoparticles Against Biofilms Formed by Clinical Strains of Pseudomonas aeruginosa Isolated from Sputum of Cystic Fibrosis Patients. Infection and Drug Resistance, 2022, Volume 15, 851-871.	2.7	4
105	Fracture mechanisms of GaAs under nanoscratching. Materials Research Society Symposia Proceedings, 2004, 841, R9.15.1.	0.1	3
106	Vibrational response of adaptive composites. European Physical Journal Special Topics, 2001, 11, Pr8-129-Pr8-134.	0.2	3
107	Quantitative imaging of diatoms by PeakForce atomic force microscopy. Surface and Interface Analysis, 2014, 46, 851-855.	1.8	2
108	Engineering the hole confinement for CdTe-based quantum dot molecules. Journal of Applied Physics, 2015, 117, .	2.5	2

#	Article	IF	CITATIONS
109	Autologous tumor‑derived microvesicles influence gene expression profiles and enhance protumorigenic chemotactic potential, signal transduction and cellular respiration in gastric cancer cells. International Journal of Oncology, 2020, 56, 359-367.	3.3	2
110	Structural and chemical properties of sputter-deposited Ti–Ge–N thin films. Surface and Coatings Technology, 2005, 200, 1483-1488.	4.8	0
111	Relaxation mechanisms in martensitic NiTi(Cu): Internal friction measurements correlated to <i>in situ</i> TEM straining. Materials Science and Technology, 2008, 24, 913-919.	1.6	0
112	Spectroscopic and positron lifetime measurements of hydrogenated single walled carbon nanohorns. Physica Status Solidi (A) Applications and Materials Science, 2016, 213, 2461-2467.	1.8	0
113	Aktivierte Modifikation der TrÃgerâ€Metallâ€Wechselwirkungen als Schlüssel für hochaktive Ru/γâ€Al 2 O 3 â€Katalysatoren für die CO x ―Methanisierung. Angewandte Chemie, 2020, 132, 22951-22959.	2.0	0